Barium and Titanium Aryl Oxides as Precursors for the Preparation of Thin-film Oxides. The Effect of Bombardment by O_2^+ †

Tomás R. Belderraín,[a] Juan P. Espinós,[a] Asunción Fernández,[a] Agustín R. González-Elipe,*[,a] Dietmar Leinen,[a] Angeles Monge,*[,b] Margarita Paneque,[a] Caridad Ruiz[b] and Ernesto Carmona*[,a]

[a] *Departamento de Química Inorgánica-Instituto de Ciencia de Materiales, Universidad de Sevilla-Consejo Superior de Investigaciones Científicas, Apdo. 553, 41071 Sevilla, Spain*

[b] *Instituto de Ciencia de Materiales, Sede D, Consejo Superior de Investigaciones Científicas, Serrano 113, 28006 Madrid, Spain and Facultad de Ciencias Químicas, Universidad Complutense, 28040 Madrid, Spain*

A set of barium aryl oxides of composition $[Ba(OC_6H_2Bu^t_2\text{-}2,6\text{-}X\text{-}4)_2(thf)_n]$ (X = H **1**, Me **2**, OMe **3** or Bu^t **4**; thf = tetrahydrofuran) has been prepared together with the related adducts $[Ba(OC_6H_2Bu^t_2\text{-}2,6\text{-}X\text{-}4)_2\{P(NMe_2)_3O\}_2]$ (X = H **5** or Me **6**), which can be obtained by treating compounds **1** and **2** with neat $P(NMe_2)_3O$ respectively. X-Ray studies showed that **6** has a distorted-tetrahedral structure, with the two Ba–O bonds to the aryl oxide ligands somewhat shorter than those to the $P(NMe_2)_3O$ groups [2.414(8) *vs.* 2.579(8) Å]. Samples of complex **4** and $[Ti(OC_6H_3Pr^i_2\text{-}2,6)_4]$, respectively, and a third homogeneous sample obtained by mixing equimolar amounts of these have been subjected to bombardment by Ar^+ and O_2^+ ions of relatively low energy (3.5 keV) and the ensuing transformation investigated by X-ray photoelectron spectroscopy. No significant variation of the C/M ratio was observed when employing Ar^+ ions, but O_2^+ produced a remarkable decrease in the carbon content which leads eventually to the formation of inorganic compounds, $BaCO_3$, TiO_2 and $BaTiO_3$, respectively, for the three samples. Action of oxygen plasma on the titanium aryl oxide did not result in a marked decrease in the C/M ratio, but it produced instead high concentrations of carbon- and oxygen-containing species.

The use of accelerated ions for the preparation and processing of different materials has experienced a remarkable development in the last few years.[1] Ion implantation, plasma etching and reactive sputtering[2,3] are some of the usual techniques for surface processing. Surface layers of oxides, carbides, nitrides, *etc.* can be obtained by ion-beam-assisted deposition, generally by using the elements as the starting materials.[4] Thin films can also be prepared by chemical vapour deposition,[5] a process which is normally stimulated by thermal activation, by plasma[6] or by a laser beam.[7] Chemical vapour deposition induced by ion beams is not a very common process, a useful application being, however, the preparation of very thin metal wires for repairing electronic circuits.[8]

Alkoxide or aryl oxide precursors[9] are widely employed for the synthesis of oxides, either by sol/gel[9b] or by chemical vapour deposition procedures.[9b] We have recently reported the preparation of oxide thin films by an ion-beam-induced chemical vapour deposition (IBICVD) method using aryl oxides as precursors.[10] The bombardment of oxides,[11] and of several types of inorganic salts[12] and oxysalts,[13] with accelerated ions has been widely investigated with the aid of various surface-sensitive techniques. The different processes induced on these materials by the bombardment has recently been comprehensively reviewed.[14] Similar studies are, however, missing for compounds such as the aryl oxides which contain a metallic element bound to an inorganic fragment. The present study is therefore aimed to clarify the type of transformations that occur when a beam of accelerated ions impinges on this type of compounds.

Barium derivatives[15] of composition $[Ba(OR)_2L_n]$ [RO = 4-X-2,6-$Bu^t_2C_6H_2O$, X = H, Me, OMe or Bu^t; L = oxygen donor, *e.g.* tetrahydrofuran (thf)] and the known compound $[Ti(OC_6H_3Pr^i_2\text{-}2,6)_4]$[16] have been chosen for this study and exposed to the action of Ar^+ and O_2^+ ions. Changes in the composition of the samples have been followed by X-ray photoelectron spectroscopy (XPS) studies. It has been found that while bombardment with Ar^+ does not alter significantly the high C/M ratio characteristic of these aryl oxide complexes, a substantial decrease of this ratio has been achieved by bombardment with O_2^+, so that this process leads, eventually, to inorganic materials. The information gained from these studies is of relevance for future applications of low-energy ion beams in the preparation of oxide films starting from volatile organometallic or co-ordination compounds. An example of this preparative procedure has been presented elsewhere.[10]

Experimental

Microanalyses were by Pascher, Microanalytical Laboratory, Remagen (Germany). Perkin-Elmer models 577 and 684 for IR and a Bruker AMX-300 spectrometer were used for NMR spectroscopy. The ^{13}C resonance of the solvent was used as internal standard, but chemical shifts are reported with respect to $SiMe_4$. Most assignments of ^{13}C NMR were supported by gated-decoupling experiments. All preparations and other operations were carried out under oxygen-free nitrogen or argon, using conventional Schlenk techniques or a dry-box.

The complex $[Ti(OC_6H_3Pr^i_2\text{-}2,6)_4]$ was prepared as described in ref. 16, from $TiCl_4$ and $Li(OC_6H_3Pr^i_2\text{-}2,6)$. A

---

† *Supplementary data available:* see Instructions for Authors, *J. Chem. Soc., Dalton Trans.*, 1995, Issue 1, pp. xxv–xxx.

Non-SI unit employed: eV ≈ 1.60×10^{-19} J.

barium rod cut into small pieces under an atmosphere of nitrogen or barium granules were used directly for the preparation of the aryl oxides $[Ba(OC_6H_2Bu^t{}_2\text{-}2,6\text{-}X\text{-}4)_2(thf)_n]$ (X = H **1**, Me **2**, OMe **3** or Bu^t **4**). A typical preparation is as follows:

In a Schlenk flask were introduced Ba (0.61 g, *ca.* 4.4 mmol) and $2,4,6\text{-}Bu^t{}_3C_6H_2OH$ (2.48 g, *ca.* 8.8 mmol) and the mixture was suspended in thf (30 cm^3), under a dinitrogen atmosphere. The alcohol dissolved and NH_3 (gas) was bubbled through the resulting mixture for 5 min. Evolution of H_2 on the surface of the metal was immediately observed. The mixture was stirred at room temperature over a period of 5 h, during which time the metal completely dissolved. A white solid precipitated upon concentration of the resulting solution but the solvent was completely removed *in vacuo* in order to eliminate the gas (NH_3 + H_2) present in the mixture. The white residue was redissolved in thf and after centrifugation a pale yellow solution was separated from a small amount of a purple solid. Concentration of the solution and cooling to −20 °C yielded colourless crystals of compound **4** (1.83 g, *ca.* 52%) which lost crystallinity upon exposure to vacuum. The remaining complexes **1**–**3** were synthesized in the form of white crystals in high yields (70–80%) following an essentially identical procedure.

Alternatively, some of the barium aryl oxides were obtained by treating the amide $[Ba\{N(SiMe_3)_2\}_2(thf)_2]$ with the corresponding phenol, as follows for compound **4**. To a solution of $[Ba\{N(SiMe_3)_2\}_2(thf)_2]$ (0.50 g, 0.83 mmol) in thf (20 cm^3) was added a solution of $2,4,6\text{-}Bu^t{}_3C_6H_2OH$ (0.43 g, *ca.* 1.66 mmol) in thf (20 cm^3). The mixture was stirred for 30 min and the solvent removed under vacuum. Extraction with thf (10 cm^3), concentration and cooling overnight to −30 °C yielded colourless crystals of **4** (0.36 g, *ca.* 54%).

$[Ba(OC_6H_3Bu^t{}_2\text{-}2,6)_2(thf)_2]$ **1** (Found: C, 61.8; H, 8.6. $C_{36}H_{58}BaO_4$ requires C, 62.5; H, 8.5%): $\delta_H(CD_2Cl_2)$ 1.50 (18 H, s, 2 Bu^t), 1.91 (4 H, m, 2 CH_2CH_2O), 3.88 (4 H, m, 2 CH_2O) and 7.05 (3 H, m, 3 aromatic CH); $\delta_C(CD_2Cl_2)$ 25.7 (s, CH_2CH_2O), 29.7 (s, CMe_3), 35.0 (s, CMe_3), 68.9 (s, CH_2O), 111.0 (br s, aromatic *p*-CH), 124.5 (s, aromatic *m*-CH) and 136.8 (s, CBu^t).

$[Ba(OC_6H_2Bu^t{}_2\text{-}2,6\text{-}Me\text{-}4)_2(thf)_2]$ **2** (Found: C, 62.6; H, 8.5. Calc. for $C_{38}H_{62}BaO_4$: C, 63.4; H, 8.7%): $\delta_H(CD_2Cl_2)$ 1.57 (18 H, s, 2 Bu^t), 1.97 (4 H, m, 2 CH_2CH_2O), 2.27 (3 H, s, Me), 3.94 (4 H, m, 2 CH_2O) and 6.91 (2 H, s, 2 aromatic CH); $\delta_C(CD_2Cl_2)$ 21.2 (s, Me), 25.7 (s, CH_2CH_2O), 30.2 (s, CMe_3), 34.9 (s, CMe_3), 68.7 (s, CH_2O), 125.0 (s, aromatic CH) and 136.5 (s, CBu^t).

$[Ba(OC_6H_2Bu^t{}_2\text{-}2,6\text{-}OMe\text{-}4)_2(thf)_3]$ **3** (Found: C, 61.1; H, 8.8. $C_{42}H_{70}BaO_7$ requires C, 61.2; H, 8.5%): $\delta_H([^2H_8]thf)$ 1.35 (18 H, s, 2 Bu^t), 1.73 (m, CH_2CH_2O), 3.57 (m, CH_2O), 3.64 (3 H, s, OMe) and 6.61 (2 H, m, 2 aromatic CH); $\delta_C([^2H_8]thf)$ 27.3 (s, CH_2CH_2O), 31.7 (s, CMe_3), 36.5 (s, CMe_3), 57.2 (s, OMe), 69.0 (s, CH_2O), 112.1 (s, aromatic CH) and 137.4 (s, CBu^t).

$[Ba(OC_6H_2Bu^t{}_3\text{-}2,4,6)_2(thf)_2]$ **4** (Found: C, 64.5; H, 9.5. $C_{44}H_{74}BaO_4$ requires C, 64.6; H, 9.6%): $\delta_H(CD_2Cl_2)$ 1.34 (9 H, s, *p*-Bu^t), 1.55 (18 H, s, 2 *o*-Bu^t), 1.92 (4 H, m, 2 CH_2CH_2O), 3.88 (4 H, m, 2 CH_2O) and 7.10 (2 H, s, 2 aromatic CH); $\delta_C(CD_2Cl_2)$ 25.7 (s, CH_2CH_2O), 30.2 (s, *o*-CMe_3), 32.1 (s, *p*-CMe_3), 35.2 (s, CMe_3), 68.6 (s, CH_2O), 121.2 (s, aromatic CH) and 135.6 (s, *o*-CBu^t).

The tris(dimethylamino)phosphine oxide complexes **5** and **6** were obtained by treating the corresponding thf adducts with $P(NMe_2)_3O$, as follows in the case of **6**. Compound **2** (0.25 g, 0.35 mmol) was dissolved in $P(NMe_2)_3O$ (0.5 cm^3) and the mixture stirred at room temperature until complete precipitation of a white solid (*ca.* 15 min). This solid was filtered off, washed with light petroleum (b.p. 40–60 °C) (3 × 10 cm^3) and dried *in vacuo*. Yield 0.23 g (85%). Crystals suitable for X-ray studies were formed by crystallization from toluene. Despite our efforts, suitable analytical data for these compounds could not be obtained. Highly crystalline samples, analytically pure according to NMR spectroscopy, provided erratic microanalyses when sent to Pascher (Remagen, Germany), sealed under vacuum. This was obviously due to decomposition of the samples under these conditions.

$[Ba(OC_6H_3Bu^t{}_2\text{-}2,6)_2\{P(NMe_2)_3O\}_2]$, **5**: $\delta_H(CD_2Cl_2)$ 1.47 (18 H, s, 2 Bu^t), 2.63 [18 H, d, $^3J(HP)$ = 9.3, $P(NMe_2)_3O$], 6.18 [1 H, t, $^3J(HH)$ = 7.5, aromatic, *p*-CH] and 6.96 [2 H, d, $^3J(HH)$ = 7.5 Hz, aromatic *m*-CH]; $\delta_C(CD_2Cl_2)$ 30.2 (s, CMe_3), 34.7 (s, CMe_3), 36.8 [d, $^2J(CP)$ = 3 Hz, $P(NMe_2)_3O$], 109.3 (s, aromatic *p*-CH), 123.9 (s, aromatic *m*-CH), 136.8 (s, aromatic CBu^t) and 167.6 (s, aromatic BaOC); $\delta_P(CD_2Cl_2)$ 24.5 (s).

$[Ba(OC_6H_2Bu^t{}_2\text{-}2,6\text{-}Me\text{-}4)_2\{P(NMe_2)_3O\}_2]$ **6**: $\delta_H(CD_2Cl_2)$ 1.57 (18 H, s, 2 Bu^t), 2.30 (3 H, s, Me), 2.73 [18 H, d, $^3J(HP)$ = 9.5 Hz, $P(NMe_2)_3O$] and 6.90 (2 H, s, aromatic CH); $\delta_C(CD_2Cl_2)$ 21.3 (s, Me), 30.3 (s, CMe_3), 34.7 (s, CMe_3), 36.9 [s, $P(NMe_2)_3O$], 117.0 (s, aromatic CMe), 124.7 (s, aromatic *m*-CH), 136.3 (s, aromatic CBu^t) and 165.2 (s, aromatic BaOC); $\delta_P(CD_2Cl_2)$ 24.7 (s).

Structure Determination of Compound **6**.—A summary of the fundamental crystal data is given in Table 1. A very unstable colourless prismatic crystal of compound **6** was introduced, under nitrogen, into a glass capillary and mounted in a kappa diffractometer. Owing to the instability of the compound, a time limit of 45 s was adopted for the final scan of a reflection. The intensities were corrected for Lorentz and polarization effects. Scattering factors for neutral atoms and anomalous dispersion corrections for Ba and P were taken from ref. 17. The structure was solved by Patterson and Fourier methods. The Ba atom was located in 2d special position. An empirical absorption correction[18] was applied at the end of the isotropic refinement. Owing to the decomposition of the crystal (decay 30%) and the non-resolvable disorder from the thermal motion of the CH_3 groups, some C atoms of these groups were refined only isotropically. In order to prevent bias on δF *vs.* F_o or $(\sin\theta)/\lambda$ weights were assigned as $w = 1/(a + b|F_o|)^2$, where a = 5.73, b = 0.05 if $|F_o| < 30$ and a = 2.2, b = 0.02 if $|F_o| \geqslant 30$. A mixed final refinement was undertaken with isotropic and anisotropic thermal parameters for the non-hydrogen atoms. The hydrogen atoms were included with fixed isotropic contributions at their calculated positions determined by molecular geometry. Final difference synthesis showed no significant electron density. Most of the calculations were carried out with the X-RAY 80 system;[19] R_F = 0.062 and R'_F = 0.064.

Additional material available from the Cambridge Crystallographic Data Centre comprises H-atom coordinates, thermal parameters and remaining bond lengths and angles.

Preparation of the XPS Samples.—Complex **4**, the known[16] $[Ti(OC_6H_3Pr^i{}_2\text{-}2,6)_4]$ and a 1 : 1 mixture of both compounds were chosen for these studies. From now on these samples will be referred to, in a simplified form, as Ba–OR, Ti–OR and Ba, Ti–OR, respectively. The mixed Ba,Ti–OR sample was obtained by mixing a solution of the Ti–OR complex (0.76 g, *ca.* 1 mmol in 10 cm^3 thf) with a solution of compound **4** (0.8 g, *ca.* 1 mmol in 10 cm^3 thf) followed by evaporation of the solvent under vacuum. For the preparation of the XPS samples the corresponding solid was placed in a dry-box and the crystals were finely powdered with the aid of a mortar and introduced into a press to form the pellets. After the sample had been pressed, a layer of heptane was carefully added on top in order to protect the sample from oxygen and humidity which could reach the material during the transfer of the pellet to the spectrometer (see below).

The XPS spectra of the aryl oxides before and after bombardment were recorded on a Leybold-Heraeus LHS-10 spectrometer; Mg-Kα radiation was used as the excitation source, with the spectrometer working in the pass-energy-constant mode at 50 eV. Calibration of the spectra was done at the C 1s peak of the hydrocarbon (*i.e.* C–H) peak taken as 284.6 eV. The spectra were stored and mathematically handled in a H-P1000E computer. The mathematical procedure consisted of background subtraction with a straight line, area calculation and fitting. In some cases the samples underwent some charging effects during recording which led to a broadening of the spectra. This could not be suppressed in a systematic way with a flood gun and all the spectra are presented as recorded, without electron bombardment.

The samples, in the form of pressed pellets, were transferred to the spectrometer in a sealed tube filled with N_2. This gas was flowed over the sample when it was transferred from the tube to the sample holder of the spectrometer. These precautions were taken to minimize the hydrolysis of these aryl oxides which are very sensitive to moisture.

The aryl oxides were subjected to bombardment with Ar^+ and $O_2{}^+$ in the pretreatment chamber of the spectrometer by means of a Penning source supplied with Ar or O_2. Typical energies of the ions were 0.5–5 keV, although most of the results presented in the following section correspond to 3.5 keV. Apart from small changes in the final C/M ratios, the ion energy did not seem to play a significant role in the control of the chemical changes induced in the targets. In most cases a current density of ions of about 15 $\mu A\ cm^{-2}$ was used and only the steady states after bombardment with Ar^+ or $O_2{}^+$ were studied. These steady states were typically reached after 20 min of sputtering. For comparison, spectra were also recorded for the Ti–OR sample exposed to a low-power plasma of oxygen. A microwave cavity supplied by a Electro-Medical generator produced the plasma inside a quartz tube connected to the preparation chamber of the spectrometer, directly onto the sample position.

Results and Discussion

Synthesis and Structural Characterization of the Aryl Oxides of Barium.—In contrast with the large amount of work devoted to the alkoxides and aryl oxides of the lanthanides,[9b,d] the corresponding complexes of the heavier alkaline-earth elements, Ca, Sr and Ba, have been almost neglected until very recently.[15] Interest in the development of new materials, including the high-T_c superconducting ceramics[20] and compounds with valuable electronic properties,[21] has significantly contributed to the rapid expansion of this area of chemistry.

Several synthetic routes are now available for the preparation of these compounds. These include the well known salt-elimination reaction from the halides MX_2 and the appropriate alkyl or aryl oxides of Li, Na or K,[22] the direct reaction of ROH with the metal in a highly reactive form[9a,23] and the ammonia-catalysed M + ROH interaction. This third route has been largely developed by Caulton *et al.*,[24] and, because of its simplicity, was chosen for the preparation of the barium aryl oxides described here [equation (1)]. An alternative procedure, which finds also literature precedent,[9d] involves the reaction of the amide $[Ba\{N(SiMe_3)_2\}_2(thf)_2]$[25] with the corresponding substituted phenol [equation (2)].

$$\mathrm{Ba(s)} + 2\,\mathrm{ROH} \xrightarrow[\mathrm{thf},\ -\mathrm{H_2}]{\mathrm{NH_3}} [\mathrm{Ba(OR)_2(thf)}_n] \qquad (1)$$

$R = 4\text{-X-2,6-Bu}^t{}_2C_6H_2$; X = H **1**, Me **2**, OMe **3** or Bu^t **4**

$$[\mathrm{Ba\{N(SiMe_3)_2\}_2(thf)_2}] + 2\,\mathrm{ROH} \xrightarrow[-\mathrm{HN(SiMe_3)_2}]{\mathrm{thf}} [\mathrm{Ba(OR)_2(thf)}_n] \qquad (2)$$

1, 3, 4

When NH_3 gas is bubbled for a few minutes through a suspension of barium granules in tetrahydrofuran containing 2 mol equivalents of the substituted phenol $4\text{-X-2,6-Bu}^t{}_2C_6H_2OH$ hydrogen evolution is observed on the surface of the metal which gradually dissolves until, after *ca.* 5 h of stirring at room temperature, a clear solution (or a whitish suspension, depending upon the concentration) is obtained. As reported by Caulton and co-workers,[25] the reaction presumably proceeds with formation of some barium amide, which then reacts with the phenol to furnish the desired aryl oxide [equation (1)]. During our work, the preparation of complex **2**, and its structural characterization by a single-crystal X-ray study, were reported.[15a,22] A complex of composition $[Ba(HOCH_2CH_2NMe_2)_4(OC_6H_3Bu^t{}_2\text{-}2,6)_2]\cdot 2C_6H_5Me$, and therefore somewhat related to **1**, has been shown[24] to contain eight-co-ordinated barium, bonded to the oxygen and nitrogen atoms of the ethanolamine ligands, with the bulky aryl oxide anions hydrogen-bonded to the OH groups of the ethanolamine ligands.

The ^1H and $^{13}C\text{-}\{^1H\}$ NMR data obtained for compounds **1**–**4** (see Experimental section) are consistent with the proposed formulation. In some cases, however, the thf content, as determined from the integration of the corresponding ^1H NMR resonances, is higher than that deduced from the microanalytical data. Since the complexes are always recrystallized from thf, or from thf-containing mixtures of solvents, this is attributed to the presence in the crystalline materials of weakly solvating tetrahydrofuran. Despite considerable efforts, additional characterization of some of these complexes by X-ray methods has proved unattainable, due to the facility with which they lose thf and crumble to white powders. However, the co-ordinated thf can be readily exchanged by other O-donors, and this has allowed the preparation of the complexes $[Ba(OC_6H_2Bu^t{}_2\text{-}2,6\text{-X-}4)_2\{P(NMe_2)_3O\}_2]$ (X = H **5** or Me **6**) containing the strongly basic hexamethylphosphoramide (hmpa) ligand [equation (3)]. Complex **6** has been characterized by spectroscopic data and additionally by X-ray studies.

$$[\mathrm{Ba(OC_6H_2Bu^t{}_2\text{-}2,6\text{-}X\text{-}4)_2(thf)_2}] \xrightarrow[-\mathrm{thf}]{\mathrm{P(NMe_2)_3O}}$$

1, 2

$$[\mathrm{Ba(OC_6H_2Bu^t{}_2\text{-}2,6\text{-}X\text{-}4)_2\{P(NMe_2)_3O\}_2}] \qquad (3)$$

5, 6

As expected for the proposed formulation, both aryl oxide ligands are equivalent and give rise to three singlets at δ 1.57 (Bu^t), 2.30 (Me) and 6.9 (aromatic CH) in the ^1H NMR spectrum. The same holds for the two $P(NMe_2)_3O$ groups, which provide a doublet at δ 2.7, with a $^3J(HP)$ coupling of 9.5 Hz. Other NMR data are collected in the Experimental section and need no further comment.

Compound **6** crystallizes from toluene as the monosolvate $[Ba(OC_6H_2Bu^t{}_2\text{-}2,6\text{-Me-}4)_2\{P(NMe_2)_3O\}_2]\cdot C_6H_5Me$. Fig. 1 shows an ORTEP[26] perspective of its molecules, including the atom numbering scheme. Relevant bond distances and angles, as well as other structural data, are collected in Tables 1–3. Since, for barium, co-ordination numbers higher than six are normal, the four oxygens surrounding the metal centre in this complex comprise an unusually low co-ordination structure. However, low co-ordination geometries are not unexpected for this element and find antecedent, for instance, in the trigonal-bipyramidal polyhedron of the closely related thf adduct $[Ba(OC_6H_2Bu^t{}_2\text{-}2,6\text{-Me-}4)_2(thf)_3]\cdot thf$[22] or in the nearly tetrahedral $[Ba\{N(SiMe_3)_2\}_2(thf)_2]$.[25a]

The Ba–O separations for the aryl oxide ligands at 2.414(8) Å are shorter than those for the $P(NMe_2)_3O$ groups [2.579(8) Å]. This is consistent with the description of the Ba–O (aryl oxide) linkages as normal covalent bonds and the Ba–O (hmpa) vectors as dative bonds.[27] The difference in length between these bonds is not too large (*ca.* 0.18 Å) and therefore the four linkages can be considered as primary, geometry-determining bonds. Both the large steric requirements of the

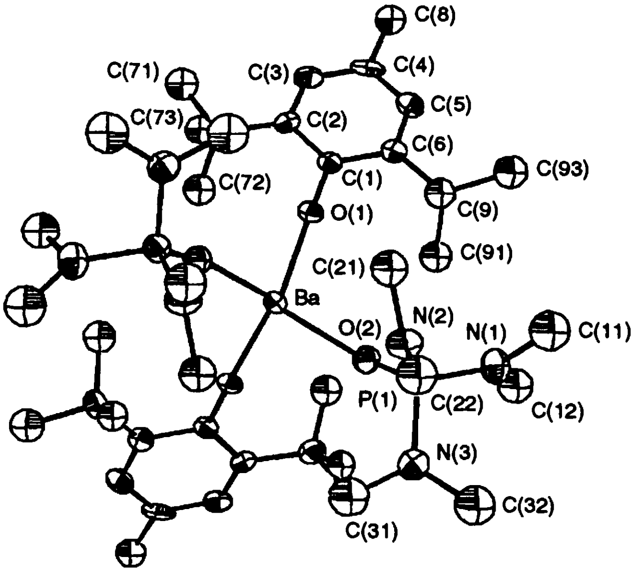

Fig. 1 An ORTEP representation of the molecular structure of complex **6** and atom labelling scheme. The ellipsoids are at 20% probability

Table 1 Crystal and refinement data for complex **6**

Formula	$C_{49}H_{90}BaN_6O_4P_2$
M	1026.6
Crystal system	Orthorhombic
Space group	*Pccn*
a/Å	18.378(2)
b/Å	14.800(4)
c/Å	21.360(5)
U/Å^3	5809(2)
Z	4
$F(000)$	2176
D_c/g cm^{-3}	1.17
T/°C	22
μ/cm^{-1}	7.77
Crystal size/mm	0.2 × 0.2 × 0.1
Diffractometer	Enraf-Nonius CAD4
Radiation	Graphite-monochromated Mo-Kα (λ = 0.710 69 Å)
Scan technique	ω–2θ
θ range/°	1–25
Data collected	(0, 0, 0) to (21, 17, 25)
Unique data	5108
Observed data [$I \geqslant 2\sigma(I)$]	2090
Standard reflections	3
R_F	0.062
R'_F	0.064
Average shift/error	0.10

Table 2 Selected bond distances (Å) and angles (°) for compound **6**

Ba–O(1)	2.414(8) × 2	C(1)–C(6)	1.41(2)
Ba–O(2)	2.579(8) × 2	C(2)–C(3)	1.38(2)
P(1)–O(2)	1.479(9)	C(2)–C(7)	1.54(2)
P(1)–N(1)	1.62(1)	C(3)–C(4)	1.35(2)
P(1)–N(2)	1.62(1)	C(4)–C(5)	1.38(2)
P(1)–N(3)	1.62(1)	C(4)–C(8)	1.52(2)
O(1)–C(1)	1.34(1)	C(5)–C(6)	1.39(2)
C(1)–C(2)	1.41(2)	C(6)–C(9)	1.54(2)
O(1)–Ba–O(2)	114.4(3) × 2	N(1)–P(1)–N(2)	109.2(6)
O(1)–Ba–O(2′)	105.2(3) × 2	O(2)–P(1)–N(3)	110.5(6)
O(1)–Ba–O(1′)	117.3(3)	O(2)–P(1)–N(2)	110.0(6)
O(2)–Ba–O(2′)	98.8(3)	O(2)–P(1)–N(1)	112.5(6)
N(2)–P(1)–N(3)	108.2(6)	Ba–O(1)–C(1)	177.6(7)
N(1)–P(1)–N(3)	106.3(7)	Ba–O(2)–P(1)	165.4(5)

Table 3 Final fractional coordinates for complex **6**

Atom	X/a	Y/b	Z/c
Ba	0.75	0.25	0.4365(0)
P(1)	0.8872(2)	0.1624(2)	0.5705(2)
O(1)	0.7956(4)	0.3773(5)	0.3778(4)
O(2)	0.8417(4)	0.1825(6)	0.5151(4)
C(1)	0.8213(7)	0.4495(8)	0.3475(6)
C(2)	0.7735(6)	0.5089(9)	0.3161(7)
C(3)	0.8011(8)	0.5806(9)	0.2820(6)
C(4)	0.8736(10)	0.5969(8)	0.2808(6)
C(5)	0.9215(7)	0.5401(9)	0.3108(7)
C(6)	0.8967(7)	0.4678(9)	0.3460(6)
C(7)	0.6909(7)	0.4936(1)	0.3186(8)
C(8)	0.9050(9)	0.6750(1)	0.2438(7)
C(9)	0.9501(7)	0.4075(0)	0.3823(6)
C(71)	0.6510(11)	0.5680(3)	0.2844(9)
C(72)	0.6733(9)	0.4051(2)	0.2897(8)
C(73)	0.6659(8)	0.4974(0)	0.3867(7)
C(91)	0.9473(9)	0.3102(2)	0.3587(8)
C(92)	0.9311(8)	0.4087(9)	0.4524(7)
C(93)	1.0302(10)	0.4377(2)	0.3795(8)
N(1)	0.9729(6)	0.1810(9)	0.5579(6)
C(11)	1.0211(11)	0.2370(6)	0.5973(9)
C(12)	1.0089(10)	0.1453(2)	0.5053(9)
N(2)	0.8605(7)	0.2227(7)	0.6298(5)
C(21)	0.8467(10)	0.3180(2)	0.6221(9)
C(22)	0.8603(9)	0.1941(2)	0.6941(9)
N(3)	0.8804(7)	0.0566(8)	0.5895(6)
C(31)	0.8140(11)	0.0085(3)	0.5803(9)
C(32)	0.9344(11)	0.0103(4)	0.6285(10)
C(40)	0.25	0.25	0.4551(13)
C(41)	0.2936(12)	0.1830(6)	0.4844(11)
C(42)	0.2901(13)	0.1862(6)	0.5439(11)
C(43)	0.25	0.25	0.5749(13)
C(44)	0.25	0.25	0.3912(0)

OR ligands and the spatial demands of the covalent, or normal bond pairs, as compared to the accepted bond pairs, make the angle subtended by the covalently bonded oxygen atoms [O(1)–Ba–O(1′) 117.3(3)°] considerably larger than that subtended by the datively bonded oxygens [O(2)–Ba–O(2′) 98.8(3)°]. These data are in agreement with those found for related complexes.[22,28]

Effect of Ion Bombardment.—Fig. 2 shows the O 1s, Ti 2p and C 1s spectra of the Ti–OR sample immediately after its transfer to the spectrometer (denoted as original, in the figure) and following bombardment with Ar^+ and $O_2{}^+$ up to the steady state. A remarkable fact, evident from this figure, is that the bombardment with $O_2{}^+$ leads to a considerable increase in the O 1s and Ti 2p intensities, as well as to a decrease in the intensity of the C 1s signal. The O 1s and Ti 2p binding energies (b.e.s) and the oxygen and titanium Auger parameters[29] obtained from these photoelectron peaks and the $KL_{23}L_{23}$ and $L_3M_{23}V$ Auger peaks respectively are summarized in Table 4. The values of these parameters obtained after sputtering with $O_2{}^+$ compare well with those reported for bulk TiO_2[30] and this clearly suggests that TiO_2 is formed after this treatment. It is also worth mentioning that in the original sample the concentration of oxygen is higher than that expected from the stoichiometry of the aryl oxide. This excess of oxygen must correspond to adsorbed water and/or hydroxyl groups. The O 1s b.e. and Auger parameter values of oxygen agree with this attribution.[30] After bombardment with Ar^+ most of this spurious oxygen is removed leading to a net increase in the intensity of the C 1s peak of the carbon beneath this first layer. A second O 1s peak at the position of TiO_2 is also observed in this case, probably because of the formation of some titanium oxide.

Figs. 3 and 4 show similar results for the Ba–OR and the Ba,Ti–OR samples, while Table 4 summarizes the b.e. and the Auger parameters of the Ba 3d, O 1s and Ti 2p levels in the

Table 4 Binding energies and modified Auger parameters for the samples subjected to different treatments

	Binding energy/eV							Modified Auger parameter/eV						
	Ti–OR		Ba–OR		Ba,Ti–OR			Ti–OR		Ba–OR		Ba,Ti–OR		
Sample treatment	O 1s	Ti $2p_{\frac{3}{2}}$	Ba $3d_{\frac{5}{2}}$	O 1s	Ba $3d_{\frac{5}{2}}$	O 1s	Ti $2p_{\frac{3}{2}}$	α'_{O}	α'_{Ti}	α'_{Ba}	α'_{O}	α'_{Ba}	α'_{O}	α'_{Ti}
Original	532.2	458.5	780.4	531.2	781.3	531.8	458.8	1039.5	—	1377.6	1040.0	1377.4	1039.8	—
Ar^+	532.2	456.5	781.2	531.8	781.2	530.8	458.0	—	—	1378.2	1040.5	1378.5	1042.1	—
O_2^+	531.0	459.3	780.5	531.3	531.8	530.8	458.7	1042.0	871.6	1377.7	1040.7	1377.6	1041.8	872.1

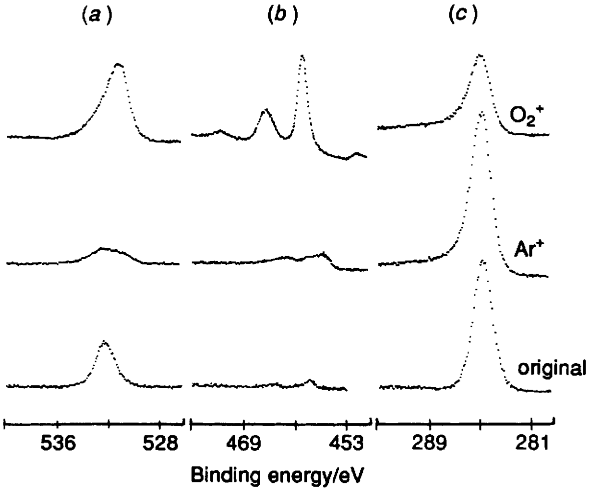

Fig. 2 The O 1s (*a*), Ti 2p (*b*) and C 1s (*c*) photoelectron spectra of Ti–OR, and of this sample subjected to sputtering with Ar^+ and O_2^+

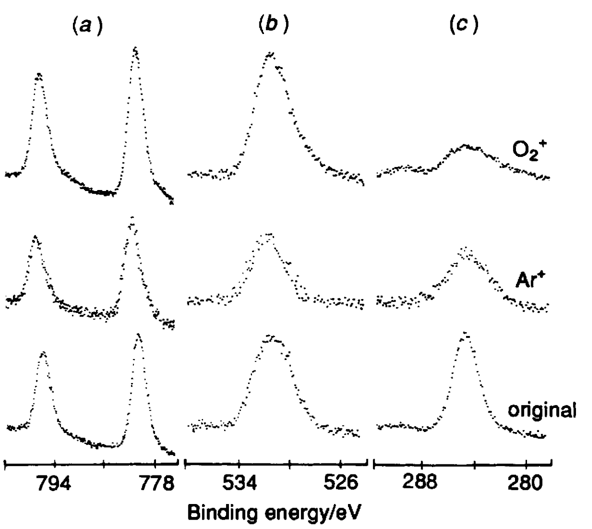

Fig. 3 The Ba 3d (*a*), O 1s (*b*) and C 1s (*c*) photoelectron spectra of Ba–OR, and of this sample subjected to sputtering with Ar^+ and O_2^+

spectra. Again, the most noticeable result is the decrease in the C 1s intensity and the increase of the O 1s, Ba 3d and Ti 2p intensities observed upon bombardment with O_2^+. Also noteworthy is the observation of a peak at *ca.* 289.5 eV in the C 1s spectrum of the Ba–OR sample. The intensity of this peak increases slightly upon exposure of the sample to CO_2, in accord with its assignment to a $BaCO_3$ compound.[31] In comparison with the spectra recorded for Ti–OR, those of Ba–OR are much broader, likely because of charging effects.

The spectra of the Ba,Ti–OR sample shown in Fig. 4 seem to be a superposition of those of Ba–OR and Ti–OR in Figs. 2 and 3, although the width of the lines is similar to that of the spectra of Ba–OR. Nevertheless, the intensity of the peak at *ca.* 289.5 eV is much smaller, indicating that a $BaCO_3$ phase is not formed in this case. During the O_2^+ bombardment experiments, CO and traces of CO_2, well above the levels usually existing in the ultra-high-vacuum chamber [*P ca.* 10^{-8} Torr (*ca.* 1.33 × 10^{-6} Pa)] could be detected by mass spectrometry.

An important observation from these studies is the preferential removal of C detected after bombardment with O_2^+. This is of relevance in connection with the use of ion-bombardment techniques for the cleaning of oxide targets[32] and for the preparation of oxide films from alkoxide precursors. With this application in mind, a quantitative evaluation of the spectra in Figs. 2–4 was effected and is presented in Fig. 5. The top of this figure shows the percentage of atoms (calculated from the areas of the photoelectron peaks) and the corresponding sensitivity factors[33] of the elements for the three situations of the sample, while the bottom part shows plots of the C/M and O/M atomic ratios. A first assessment of the values in this figure evidences that, in comparison to the stoichiometric C/M ratios in the pure aryl oxide (48 and 30:1, respectively, for the Ti–OR and the Ba–OR samples), those calculated by XPS present a considerable deviation, specially in the case of the barium aryl oxide sample. As already mentioned, this difference must be due to surface contamination of the samples by hydrolysis during transfer to the XPS spectrometer. Fig. 5 shows that this hydrolytic process is particularly important for the barium aryl oxide, in excellent accord with the chemical behaviour found for this compound.

Bombardment with Ar^+ produces a decrease in the C/M ratio in the two aryl oxides, but bombardment with O_2^+ is much more effective in preferentially removing the C 1s. Thus, for the three samples the steady state reached after this treatment is characterized by a C/M ratio of approximately 3:1 and an O/M ratio of between 2 and 3:1. This means that the bombarded targets are formed by *ca.* 50% C and 50% of atoms of the metal oxides or carbonates (see top part of Fig. 5), which unambiguously demonstrates the effectiveness of bombardment by O_2^+ for preferential removal of C from targets containing inorganic and organic elements. Recall in this respect that for the Ti–OR sample the C/M ratio decreases from 48 to 3:1.

In order to gain some information about the mechanism of this process the Ti–OR sample was exposed to an oxygen plasma. Similar experiments were not carried out with the Ba–OR and the Ba,Ti–OR samples because their photoelectron spectra are wide and the fitting analysis would not provide any valuable information in this regard. Fig. 6 shows the spectra recorded for this sample before and after the experiment. While the intensity of the Ti 2p peak does not increase significantly after the plasma treatment, that of the O 1s peak does increase. It is also interesting that the steady-state Ti 2p b.e. coincides with that obtained after bombardment by O_2^+ (*i.e.* 459.5 eV), whilst the O 1s peak appears at 532.8 eV, as compared to the 531.0 eV in the O_2^+ experiment (see Table 4). In addition, the C 1s peak also decreases in intensity and changes its shape with the appearance of a well defined peak at 289.5 eV.

A fitting analysis of the O 1s and C 1s peaks of the Ti–OR

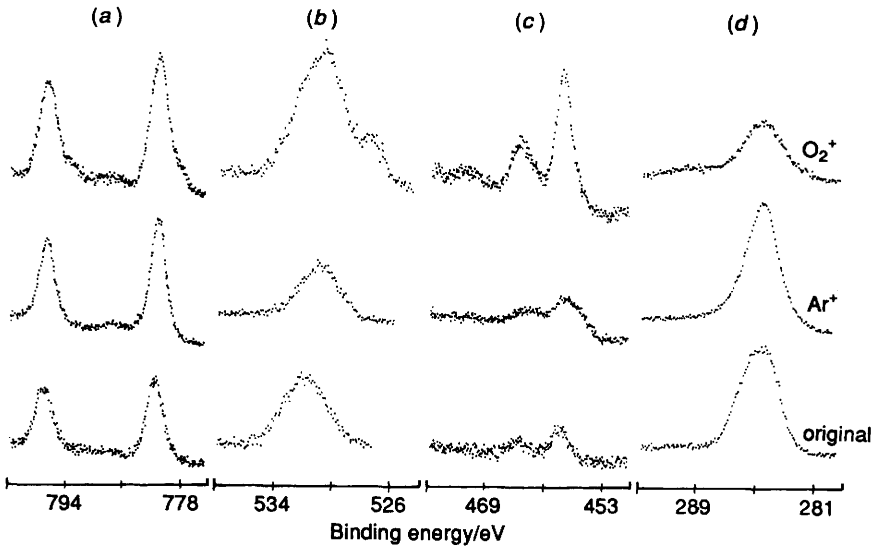

Fig. 4 The Ba 3d (*a*), O 1s (*b*), Ti 2p (*c*) and C 1s (*d*) photoelectron spectra of Ba,Ti–OR and of this sample subjected to sputtering with Ar^+ and O_2^+

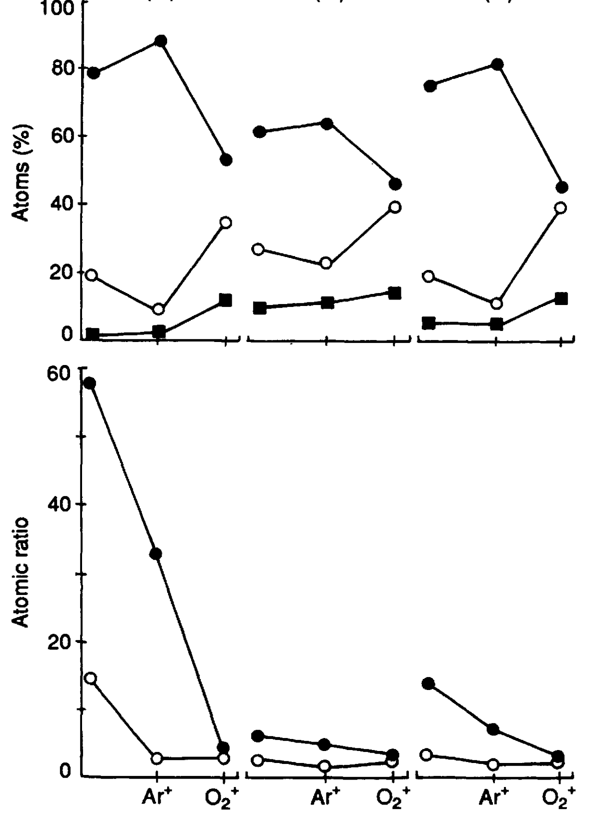

Fig. 5 Top: atomic percentages (■, M; ●, C; ○, O; calculated from the XPS spectra) of the aryl oxides Ti–OR (*a*), Ba–OR (*b*) and Ba, Ti–OR (*c*) after introduction in the ultra-high-vacuum chamber and after sputtering with Ar^+ and O_2^+. Bottom: Atomic ratios (●, C/M; ○, O/M) for the same situations of the samples

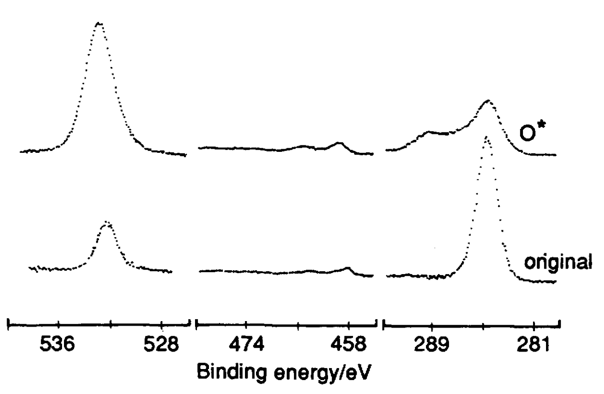

Fig. 6 The O 1s (*a*), Ti 2p (*b*) and C 1s (*c*) photoelectron spectra of Ti–OR, and of this sample after exposure to an oxygen plasma of low intensity

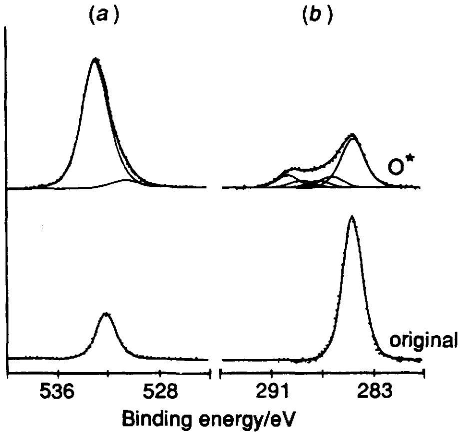

Fig. 7 Fitting of the O 1s (*a*) and C 1s (*b*) photoelectron spectra of Ti–OR before and after exposure to the oxygen plasma (*i.e.* spectra of Fig. 6)

sample in its original form and after exposure to an oxygen plasma is shown in Fig. 7. Fitting of the C 1s peak after the plasma treatment was carried out with five peaks displaying b.e.s at 284.6, 286.2, 287.3, 288.0 and 289.0, which in the literature on carbon–oxygen functional groups are usually attributed to different chemical states ranging from the non-oxygen-containing product, *i.e.*–C–C–, to the fully oxygenated species, –C(O)O–.[34] The O 1s peak in this case consists of a single component at 532.0 eV with a small contribution at 530.0 eV. The first one is likely due to the carbon-bound oxygen in these functional groups. This is supported by the intensities of this oxygen peak and those of the carbon peaks corresponding to oxygen-containing species, which after modification by their sensitivity factors yield similar atom concentrations. Following an analogous procedure, the fitting in Fig. 8 of the O 1s and C 1s

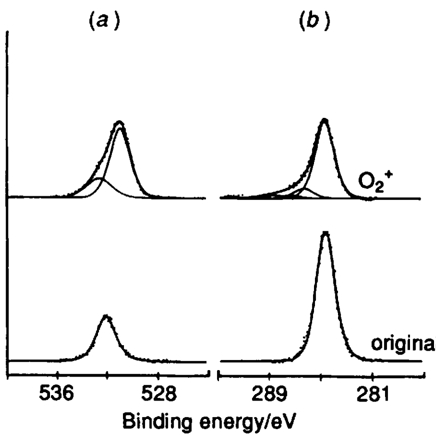

Fig. 8 Fitting of the O 1s (*a*) and C 1s (*b*) photoelectron spectra of Ti–OR before and after bombardment with O_2^+ (*i.e.* spectra of Fig. 2)

peaks after bombardment by O_2^+ indicates that the concentration of carbon atoms associated with oxygen is much smaller. In a parallel way the O 1s band at 532.0 eV is also smaller, as expected if this band corresponds to the C–O species. Therefore, the very intense O 1s band at 530.0 eV must be associated with the Ti 2p peak, which after bombardment by O_2^+ was also very intense. The evaluation of these intensities, modified by the intensity factors of O and Ti, gives an O/Ti ratio of approximately 2:1.

The results described above clearly show that the bombardment of complex targets, formed by organic molecules and inorganic elements (M), with Ar^+ ions, does not alter significantly the C/M ratio, while the use of O_2^+ produces a sharp decrease in the carbon content and leads eventually to the formation of inorganic compounds. Thus, TiO_2 is formed when using an aryl oxide complex of Ti as a precursor and $BaCO_3$ results if a Ba–OR target is employed instead. The latter result is consistent with the fact that BaO would yield the carbonate in the presence of CO_2 and that CO and/or CO_2 are formed during bombardment of the organic matrix with O_2^+. As will be discussed below, the formation of these molecules is critical in the mechanism that leads to the observed enrichment of the target in the inorganic compound. Interestingly, carbonate formation is not detected during bombardment of the Ba,Ti–OR sample. A plausible explanation is the formation in this case of a barium titanate, stable toward action of CO_2.

A comparison of the experiments carried out with O_2^+ and the oxygen plasma with the Ti–OR sample provides a clue as to why bombardment with O_2^+ produces the observed decrease in the C/M ratio of the target. Such a diminution is not observed in the plasma assay, in which, contrary to the above, high concentrations of carbon- and oxygen-containing species are detected. A C 1s photoelectron spectrum similar to that obtained in our case with the plasma (*cf.* Figs. 6 and 7) has been observed by McIntyre *et al.*[32] when trying to remove hydrocarbon overlayers from a SiO_2 substrate by ultraviolet/ozone exposure. During the bombardment by O_2^+, carbon–oxygen species are also formed, although in much smaller concentrations than found in the experiment with the oxygen plasma. To explain this difference it can be reasonably argued that such species would yield CO_2 very readily under bombardment, and furnish in this fashion an alternative route for the preferential sputtering of C. This route does not exist in the experiments with Ar^+ ions, where C is sputtered away without oxygen from the C–H matrix.

Lastly it should be stressed that the aforementioned results suggest that the final C/M ratio of *ca.* 3:1 found for the three aryl oxide precursors discussed, *viz.* Ba–OR, Ti–OR and Ba,Ti–OR, could be reduced appreciably by using precursors that exhibit a lower carbon content. Evidence in this direction has already been provided by related work from our laboratories dealing with the preparation of a TiO_2 thin film by the IBICVD procedure.[10,35]

Acknowledgements

We gratefully acknowledge generous support from the Comisión Interministerial de Ciencia y Tecnología (Proyecto MAT91-0379) and the Junta de Andalucía. D. L. and T. R. B. thank the E.C. (Science program) and the Spanish Ministry of Education (MEC), respectively, for a research grant. Thanks are also due to the University of Sevilla for the use of its analytical and NMR facilities.

References

1 *Handbook of Ion Beam Processing Technology*, eds. J. J. Cuomo, N. S. Rossnagel and H. R. Kaufman, Noyes, Park Ridge, New Jersey, 1989.
2 *Ion Bombardment Modification of Surfaces*, eds. O. Auciello and R. Kelly, Elsevier, Amsterdam, 1984.
3 F. A. Smidt and G. K. Hubler, *Nucl. Instrum. Methods*, 1993, **B80/81**, 207.
4 K. G. Wolf, *J. Vac. Sci. Technol.*, 1992, **A10**, 1757.
5 A. G. Zawadzki, C. J. Giunta and R. G. Gordon, *J. Phys. Chem.*, 1992, **96**, 4364.
6 A. D. Huelsman and R. Reif, *J. Vac. Sci. Technol.*, 1989, **A7**, 2554.
7 M. Ishida, A. Eto and T. Nakamura, *J. Vac. Sci. Technol.*, 1989, **A7**, 2931.
8 T. Tao, W. Wilkinson and J. Melngailis *J. Vac. Sci. Technol.*, 1991, **B9**, 162.
9 (*a*) D. C. Bradley, R. C. Mehrotra and D. P. Gaur, *Metal Alkoxides*, Academic Press, London, 1978; (*b*) D. C. Bradley, *Chem. Rev.*, 1989, **89**, 1317; (*c*) R. C. Mehrotra, *Adv. Inorg. Chem. Radiochem.*, 1983, **26**, 269; (*d*) K. G. Caulton and L. G. Hubert-Pfalzgraf, *Chem. Rev.*, 1990, **90**, 969.
10 D. Leinen, J. P. Espinós, A. Fernández and A. R. González-Elipe, *J. Vac. Sci. Technol.*, 1994, **A12**, 2728.
11 J. B. Malherbe, S. Hofmann and J. M. Sanz, *Appl. Surf. Sci.*, 1986, **27**, 355; A. R. González-Elipe, J. P. Espinós, G. Munuera and J. M. Sanz, *Surf. Sci.*, 1989, **220**, 368.
12 S. Adurn, S. Contarini and J. W. Rabalais, *J. Phys. Chem.*, 1986, **90**, 1683; A. B. Christie, J. Lee, I. Sutherland and J. M. Walls, *Appl. Surf. Sci.*, 1983, **15**, 224.
13 S. F. Ho, S. Contarini and J. W. Rabalais, *J. Phys. Chem.*, 1987, **91**, 4779.
14 R. Kelly, *Mater. Sci. Eng.*, 1989, **A115**, 11.
15 (*a*) P. B. Hitchcock, M. F. Lappert, G. A. Lawless and B. Royo, *J. Chem. Soc., Chem. Commun.*, 1990, 1141; (*b*) K. G. Caulton, M. H. Chisholm, S. R. Drake and K. Folting, *J. Chem. Soc., Chem. Commun.*, 1990, 1349; (*c*) F. G. N. Cloke, P. B. Hitchcock, M. F. Lappert, G. A. Lawless and B. Royo, *J. Chem. Soc., Chem. Commun.*, 1991, 724; (*d*) K. F. Tesh and T. P. Hanusa, *J. Chem. Soc., Chem. Commun.*, 1991, 879; (*e*) K. G. Caulton, M. H. Chisholm, S. R. Drake and J. C. Huffman, *J. Chem. Soc., Chem. Commun.*, 1990, 1498; (*f*) O. Poncelet, L. G. Hubert-Pfalzgraf, L. Toupet and J. C. Daran, *Polyhedron*, 1991, **10**, 2045; (*g*) S. R. Drake, D. J. Otway, M. B. Hursthouse and M. A. Abdul, *Polyhedron*, 1992, **11**, 1995; (*h*) K. G. Caulton, M. H. Chisholm, S. R. Drake, K. Folting and J. C. Huffman, *Inorg. Chem.*, 1993, **32**, 816; (*i*) K. F. Tesh, D. J. Burkey and T. P. Hanusa, *J. Am. Chem. Soc.*, 1994, **116**, 2409.
16 L. D. Durfee, S. L. Latesky, I. P. Rothwell, J. C. Huffman and K. Folting, *Inorg. Chem.*, 1985, **24**, 4569.
17 *International Tables for X-Ray Crystallography*, Kynoch Press, Birmingham, 1974, vol. 4, p. 72.
18 N. Walker and D. Stuart, *Acta Crystallogr., Sect. A*, 1983, **39**, 158.
19 J. M. Stewart, The X-RAY 80 System, Computer Science Center, University of Maryland, College Park, MD, 1985.
20 C. N. R. Rao and B. Raveau, *Acc. Chem. Res.*, 1989, **22**, 106.
21 L. G. Hubert-Pfalzgraf, *New J. Chem.*, 1987, **11**, 663.
22 K. F. Tesh, T. P. Hanusa, J. C. Huffman and C. J. Huffman, *Inorg. Chem.*, 1992, **31**, 5572.
23 M. J. McCormick, K. B. Moon, S. R. Jones and T. P. Hanusa, *J. Chem. Soc., Chem. Commun.*, 1990, 778.
24 K. G. Caulton, M. H. Chisholm, S. R. Drake and K. Folting, *Inorg. Chem.*, 1991, **30**, 1500.
25 (*a*) B. A. Vaartstra, J. C. Huffman, W. E. Streib and K. G. Caulton,

Inorg. Chem., 1991, **30**, 121; (*b*) D. C. Bradley, M. B. Hursthouse, A. A. Ibrahim, K. M. A. Malik, M. Motevalli, R. Möseler, H. Powell, J. D. Runnacles and A. C. Sullivan, *Polyhedron*, 1990, **9**, 2959.

26 C. K. Johnson, ORTEP, Report ORNL-5138, Oak Ridge National Laboratory, Oak Ridge, TN, 1976.

27 A. Haaland, *Angew. Chem., Int. Ed. Engl.*, 1989, **28**, 992.

28 R. L. Geerts, J. C. Huffman and K. G. Caulton, *Inorg. Chem.*, 1986, **25**, 1803.

29 C. D. Wagner, *Faraday Discuss. Chem. Soc.*, 1975, **60**, 291.

30 A. Fernández, A. Caballero and A. R. González-Elipe, *Surf. Interf. Anal.*, 1992, **18**, 392.

31 A. R. González-Elipe, J. P. Espinós, A. Fernández and G. Munuera, *Appl. Surf. Sci.*, 1990, **45**, 103.

32 N. S. McIntyre, R. D. Davidson, T. L. Walzak, R. Williston, M. Westcott and A. Pekarsky, *J. Vac. Sci. Technol.*, 1991, **A9**, 1355.

33 *Practical Surface Analysis*, eds. D. Briggs and M. P. Seah, Wiley, Chichester, 1990, vol. 1.

34 G. P. López, D. G. Castner and B. D. Ratner, *Surf. Interf. Anal.*, 1991, **17**, 267.

35 D. Leinen, A. Fernández, J. P. Espinós, T. R. Belderraín and A. R. González-Elipe, *Thin Solid Films*, 1994, **241**, 198.

Received 8*th December* 1994; *Paper* 4/07498J